ORIGINAL ARTICLE

lajss.org© Latin American Journal of Solids and Structures

www.lajss.org

A Multimodal Deep Learning Method for Inverse Design of Occupant Restraint Systems

Hongbin Tang[a,b], **Ledan Liu**[a,b], **Jian Xie**[c*]

[a] National key Laboratory of Advanced Vehicle Integration and Control, Changchun, China. Email: tanghongbin@faw.com.cn
[b] FAW Global R&D Center, Changchun, China.
[C] Jilin University, Changchun, China. Email: xiejian@jlu.edu.cn

* Corresponding author

https://doi.org/10.1590/1679-7825/e9237

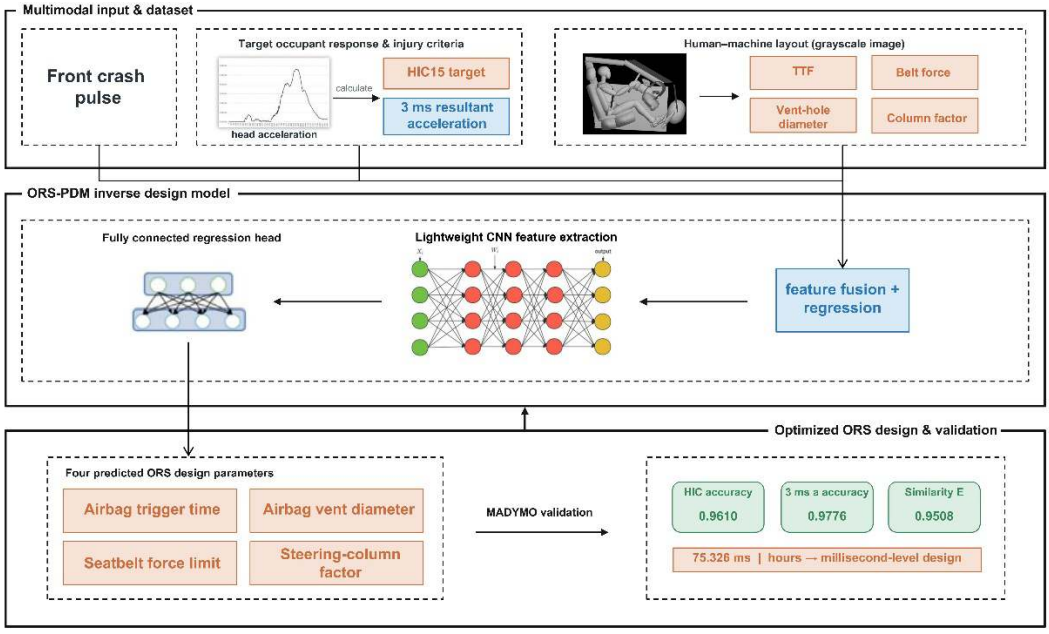
Abstract

The design of occupant restraint system (ORS) parameters is directly related to the crash safety performance of vehicles. However, traditional iterative simulation and manual parameter tuning methods suffer from long design cycles and high computational costs, while existing deep learning methods mostly focus on indirect modeling or injury prediction, lacking direct parameter design capability for multimodal data. To address this issue, this paper proposes a CNN-based ORS parameter inverse design model (ORS-PDM) that achieves unified input and joint representation of three types of multimodal parameters: time-series, image, and numerical data. Specifically, the crash pulse (time-series modality), the grayscale image of the human-machine layout (image modality), and the HIC metric (numerical modality) are taken as heterogeneous inputs. After unified preprocessing, these data are encoded into tensor channels and concatenated at the channel level, and then fed into the network to directly predict the optimal ORS parameter combination, thereby realizing inverse parameter design.

Keywords

occupant restraint system, inverse design, multimodal deep learning, occupant protection, vehicle collision

Graphical Abstract



Received August 17, 2026. In revised form August 18, 2026. Accepted September 03, 2026. Available online September 09, 2026.
https://doi.org/10.1590/1679-7825/e9237

Latin American Journal of Solids and Structures. ISSN 1679-7825. Copyright © **2026**. This is an Open Access article distributed under the terms of the Creative Commons Attribution License, which permits unrestricted use, distribution, and reproduction in any medium, provided the original work is properly cited.

1. INTRODUCTION

The occupant restraint system (ORS) is a core component of a vehicle's collision safety system, and the quality of its design is directly related to the vehicle's protective performance during crash events. The ORS mitigates collision forces and reduces occupant injuries through the coordinated operation of multiple subsystems, including seat belts, airbags, seating systems, instrument panels, and steering mechanisms. Each of these subsystems exhibits complex mechanical and physical behaviors, with dynamic responses that are highly nonlinear and mutually coupled, thereby increasing the difficulty and complexity of ORS parameter design.

Moreover, the inputs to the ORS—namely vehicle acceleration and structural deformation—are inherently random and unpredictable, while the outputs include occupant responses and injury evaluation metrics. These physical responses exhibit significant spatial variations across different body regions and involve multiple spatial directions (e.g., X, Y, and Z). As a result, the input–output relationship of the ORS cannot be formulated as a deterministic function. The parameters of the ORS are characterized by high. nonlinearity and significant noise sensitivity, further complicating the design process ,as shown in Figure 1.

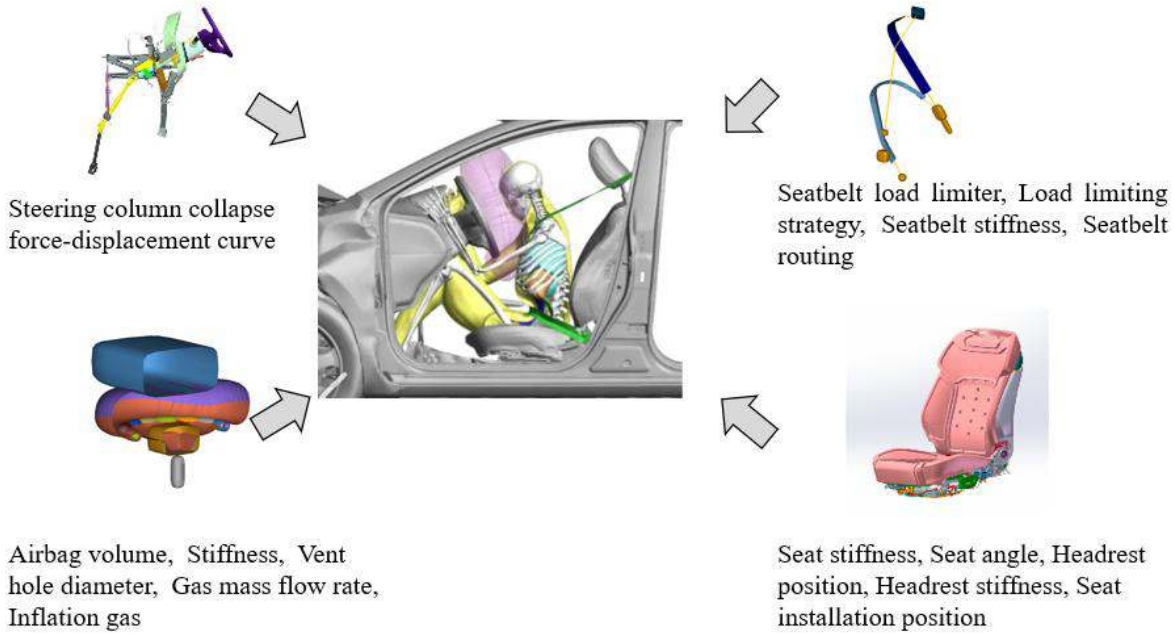


Figure 1 Design parameters of ORS.

To address the challenges associated with ORS parameter design and matching, researchers have long employed numerical simulation methods to assess the influence of various design parameters on occupant injury outcomes. With advances in computational technology, surrogate modeling techniques have been widely adopted in the optimization of vehicle restraint systems. For example, Gu et al.Itegrated the Kriging method with the Non-dominated Sorting Genetic Algorithm II (NSGA-II) to perform multi-objective optimization of ORS parameters. Horii applied response surface methodology (RSM) in conjunction with an evolutionary algorithm to optimize multiple competing objectives in ORS design. Yang et al.developed a surrogate model based on radial basis functions(RBFs), incorporating critical injury metrics across various body regions, and combined it with NSGA-II to systematically match and optimize ORS parameters.

With the maturation of machine learning (ML) theory, its applications have expanded rapidly in fields such as structural engineering,occupant injury prediction, and traffic accident risk assessment. In the context of ORS design, ML techniques have been used to construct surrogate models for optimal parameter selection or to evaluate the reasonableness of restraint system configurations by predicting injury outcomes. For instance, Heo et al. developed a machine learning framework to predict Euro NCAP injury scores of dummies under various ORS configurations. Zhang et al. employed a hybrid LSTM-FFNN model to predict whiplash injury responses based on simulation data, enabling rapid evaluation of seat design variables and enhancing development efficiency.

While ML-based methods have demonstrated promising capabilities in ORS design and evaluation, most existing studies focus on indirect modeling or injury prediction rather than the direct generation of optimized restraint system parameters. As such, a systematic and real-time solution for direct ORS parameter design remains underexplored.

To bridge this gap, this study proposes a novel, intelligent design framework based on ShuffleNet V2 for the direct prediction and matching of ORS parameters. The proposed method, referred to as the Occupant Restraint System Parameter Design Model (ORS-PDM), accelerates the design process by mapping target occupant response signals to optimal ORS configurations. In addition, several convolutional neural network (CNN) architectures are comparatively evaluated for this task, and experimental results demonstrate that ShuffleNet V2 achieves the highest prediction accuracy with the shortest training time, making it particularly suitable for real-time or resource-constrained deployment.

2. Methodology

In order to quickly design the ORS parameters and realize the intelligent design of vehicles, this paper proposes a lightweight CNN-based method. Specifically, this paper establishes the Occupant Restraint System Parameter Design Model (hereafter referred to as ORS-PDM), which realizes the prediction of head acceleration to the combination of restraint system parameters. Figure 2 shows the research framework of the proposed method, which is divided into the following three steps (i.e., dataset establishment, ORS-PDM, and result analysis). The general steps of the proposed method are described below.

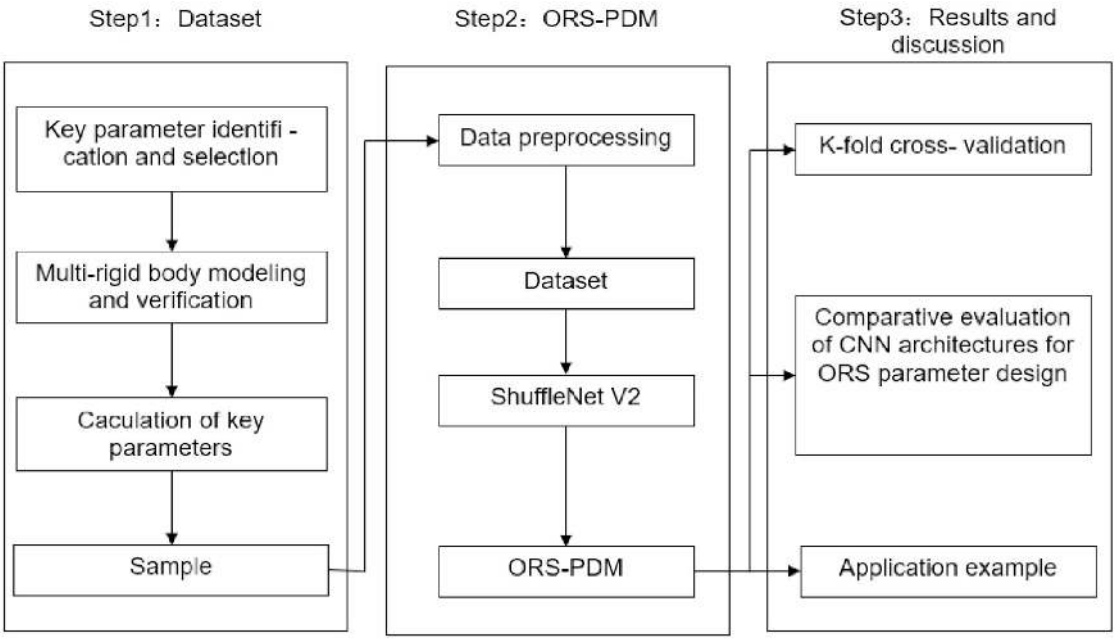


Figure 2 Research framework.

To enable rapid and intelligent design of ORS parameters, this study proposes a lightweight prediction method based on ShuffleNet V2. Specifically, an ORS-PDM is developed to directly predict an optimal combination of ORS parameters from a given head acceleration–time curve. The overall research framework is illustrated in Figure 2, and comprises three main steps (i.e., dataset, ORS-PDM, and results and discussion). The methodology is summarized as follows:

Step 1: Key occupant injury assessment indicators and influencing factors were identified, and the parameter space was defined. Latin hypercube sampling (LHS) was employed to generate parameter combinations, followed by multi-rigid body simulations to obtain occupant injury responses.

Step 2: The ShuffleNet V2 architecture was constructed and optimized by selecting appropriate hyperparameters. To ensure efficient and accurate model input, data preprocessing was performed, including normalization and formatting of multi-modal features. The model's generalization performance was evaluated through k-fold cross-validation, providing insight into its robustness across different data partitions.

Step 3: The generalization ability and stability of the ORS-PDM were assessed using five-fold cross-validation. To further validate its effectiveness, ShuffleNet V2 was compared with both deeper CNN models (e.g., ResNet18/50) and other lightweight architectures (e.g., MobileNet V2). These comparisons demonstrated the superior balance between efficiency and accuracy achieved by ShuffleNet V2. In addition, an application case based on Vehicle A was conducted to verify the model's performance in a real-world engineering scenario.

3. DATASET

A high-quality, diverse, and well-structured dataset is critical to the success of any ML model, as it directly influences the training efficiency and prediction accuracy. To support the development of the ORS-PDM proposed in this study, a comprehensive dataset was constructed, incorporating occupant responses, key restraint system parameters, and relevant influencing factors under frontal crash.

3.1 Dataset Construction

3.1.1 Determination of Design Variables

The configuration of ORS parameters has a direct impact on occupant injury severity. Among various injuries, head-related trauma ranks as the leading cause of fatalities in traffic accidents. Consequently, head injury criteria have become essential indicators in vehicle safety regulations across numerous countries. Previous studies have shown that head acceleration is a key biomechanical factor causing traumatic brain injury. To capture this dynamic response, this study adopts the occupant head acceleration-time curve as the main input parameter of the model.

The four finally determined ORS design variables and their value ranges are listed in Table 1. It should be noted that these value ranges are applicable to the vehicle platform and simulation configuration selected in this study, and may not be applicable to all vehicle models; however, they are sufficient to serve as a baseline for verifying the feasibility and effectiveness of the proposed method.

Table 1. Selected ORS parameters

Parameter	expressions
Airbag trigger time (TTF) [ms]	value
Airbag vent diameter [mm]	value
Seatbelt force [N]	Curve
Steering column crush force-displacement curve	Curve

3.1.2 Input Data

The degree of occupant injury is influenced by various parameters in the entire vehicle-occupant system, including the crashworthiness of the vehicle, the parameters of the restraint system, and the human-machine layout parameters of the vehicle's interior.

1. Front crash pulse

During a frontal collision, the vehicle's front-end structure deforms to absorb impact energy and mitigate occupant injury. The acceleration measured at the B-pillar is commonly used as a representative signal of crash severity and is typically referred to as the vehicle's "front crash pulse," which can characterize the dynamic loading conditions during a frontal collision. The front crash pulse reflects the vehicle's mass, energy absorption capacity, and structural stiffness, is closely related to injury outcomes, and varies across different vehicle platforms. As shown in Figure 3, the front crash pulse can serve as a comprehensive indicator of impact dynamics and is used as the main loading input in this study.

2. HIC

China's New Car Assessment Program (C-NCAP, 2024) quantifies head injury severity using indices derived from acceleration curve as shown is Figure4. Namely, the Head Injury Criterion (HIC_{15}) and the 3 ms resultant acceleration. These metrics serve as vital references in model evaluation. The calculation formula of HIC_{15} is shown in Equation 1:

$$\mathrm{HIC}_{15} = \max\left\{(\mathrm{t}_2 - \mathrm{t}_1)\left[\frac{1}{\mathrm{t}_2-\mathrm{t}_1}\int_{\mathrm{t}_1}^{\mathrm{t}_2}\frac{\mathrm{a}}{\mathrm{g}}\mathrm{dt}\right]^{2.5}\right\} \quad (1)$$

where a represents the acceleration response value of the head during the collision process; g denotes the gravitational acceleration; t_1 and t_2 represent two moments during the collision process, with the maximum time interval not exceeding 15 ms. This means that within a time interval from t_1 to t_2 (not exceeding 15 ms), the maximum value of the HIC formula over that specific interval can be obtained.

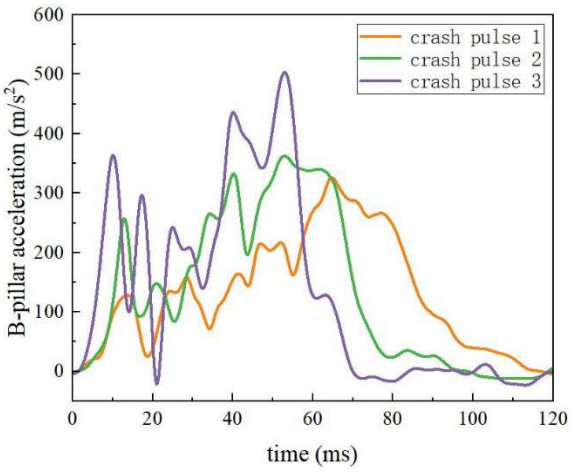


Figure 3 Front crash pulse.

3. Human-machine layout parameters

The interior layout affects not only occupant ergonomics but also crash safety performance. While certain constraints (e.g., H-point and pelvic angle) are defined by regulatory standards such as C-NCAP, there is still optimization space in the positioning of the steering column, dashboard, airbag, seatbelt anchor points, and headrest. These spatial factors directly affect occupant kinematics and injury severity after a collision. However, measuring and representing each of the above layout parameters individually in numerical form is not only numerous and cumbersome, but also susceptible to measurement errors and subjective judgment, and it is difficult to fully reflect the geometric morphology and spatial relationships among components. To this end, this study encodes the interior layout information as a grayscale image—using pixel intensity to represent the presence or absence of structures, comprehensively presenting the multidimensional spatial configuration of the steering column, dashboard, airbag, seatbelt anchor points, headrest, and occupant posture. This grayscale map of spatial parameters as shown in Figure 4 serves as the image modality input, and together with the time-series and numerical modalities such as the front crash pulse and HIC metric, constitutes the multimodal input of the model.

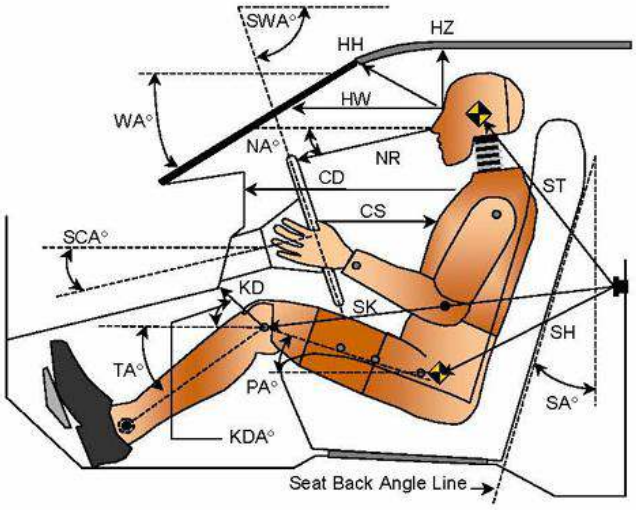


Figure 4 Interior layout of the cockpit (left side view).

3.2 Unified Preprocessing and Joint Representation of Multimodal Data

The above dataset involves three types of heterogeneous data: time-series, numerical, and image. The front crash pulse and head acceleration-time curve are time-series input signals, the human-machine layout is a grayscale image input, and the four ORS design parameters are scalar numerical outputs (i.e., the supervisory signals of the model).

Among them, the time-series and image input modalities differ significantly in dimension, length, and data structure, and cannot be directly fed into a neural network for joint modeling. To this end, this section proposes a unified preprocessing pipeline: the time-series and image inputs are separately formatted and normalized, converted into tensor channels of consistent size, and a joint representation is constructed based on channel-level concatenation; meanwhile, the four ORS parameters serving as supervision are min-max normalized to bring them to the same scale as the input features. After the above processing, a single lightweight convolutional network can simultaneously perceive temporal dynamics and spatial structure within its receptive field, and take the normalized numerical parameters as regression targets, thereby collaboratively utilizing multi-source information to complete parameter design.

3.2.1 Time-Series Data Preprocessing

The front crash pulse and head acceleration-time curve retain their original time-series format to fully preserve their temporal dynamic characteristics. The preprocessing of time-series data consists of two steps:

1. Time-axis alignment and resampling. The simulation duration and sampling frequency differ across samples. To form fixed-size input tensors, all time-series signals need to be uniformly resampled to the same number of sampling points and aligned on the time axis.
2. Min-max normalization. To eliminate dimensional differences and ensure numerical stability, each time-series signal is normalized according to Equation 2:

$$\mathrm{X_{Norm}} = \frac{\mathrm{X_i} - \mathrm{X_{min}}}{\mathrm{X_{max}} - \mathrm{X_{min}}} \tag{2}$$

Where, X_i is the original data, X_{Norm} is the normalized data, X_{max} and X_{min} are the maximum and minimum values of the data respectively.

3.2.2 Numerical Data Preprocessing

The numerical variables in the dataset are the four ORS design parameters, (i.e., the supervisory outputs of the model). To bring them to the same scale as the input features and ensure stable training, each parameter is also min-max normalized using Equation 2, mapping to [0, 1]; the predicted parameter values output by the model are inverse-normalized back to physical dimensions before being fed into the multi-rigid body simulation for validation.

3.2.3 Image Data Preprocessing

Spatial information such as seatbelt anchor positions, occupant posture, and interior layout involves numerous components and complex geometric relationships. Representing each item with numerical coordinates is not only cumbersome to measure, but also susceptible to measurement errors and subjective judgment, and it is difficult to fully reflect the spatial topological relationships among components. To this end, this study uniformly encodes the above spatial information as grayscale images: based on a Python script, the geometric contours and positions of key components such as the steering column, dashboard, airbag, seatbelt anchor points, seat, and dummy posture in the MADYMO multi-rigid body model are automatically read, and after grayscale processing, output as single-channel bmp format images. In this grayscale image, pixel intensity only represents the "presence" or "absence" of a structure—regions occupied by structures take high grayscale values, and background regions take low grayscale values; the grayscale itself carries no additional physical dimension, thereby comprehensively presenting the multidimensional spatial configuration in a compact two-dimensional matrix form. Image preprocessing consists of the following three steps:

3. Resolution unification: The grayscale images generated by different samples may have size differences. All images need to be adjusted to a unified resolution of 35×35 through interpolation to ensure consistent input tensor size and facilitate subsequent channel-level concatenation with the time-series channels.
4. Pixel intensity normalization: The pixel value range of original bmp images is the integer [0, 255]. To bring them to the same scale as the time-series and numerical modalities and ensure training stability, min-max normalization consistent with Equation 2 is applied to map pixel intensity to the [0, 1] interval.
5. Channel dimension expansion: The normalized grayscale image is a single-channel two-dimensional matrix. To align with the time-series channels in terms of dimensions, it is expanded in the channel dimension into a tensor of shape 1×35×35 to participate in the channel-level concatenation in Section 3.2.4.

The processed grayscale map of spatial parameters is shown in Figure 5.

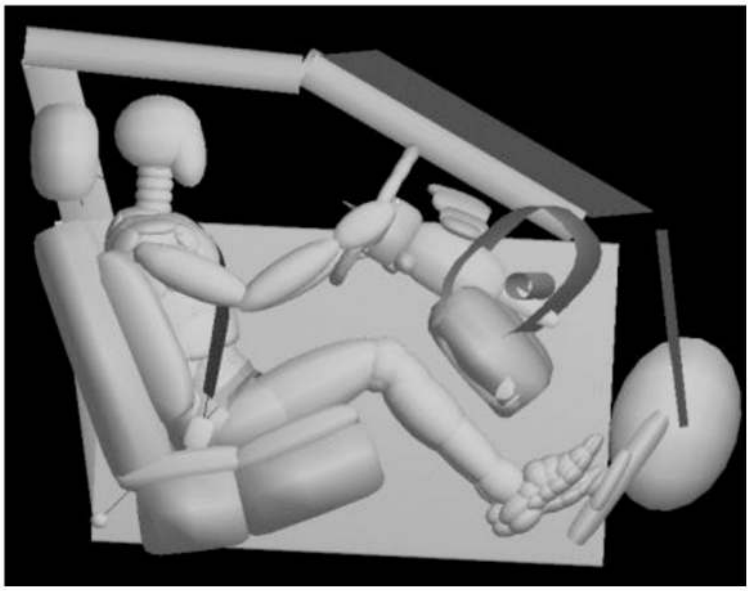


Figure 5 Grayscale map of spatial parameters.

4. OCCUPANT RESTRAINT SYSTEM PARAMETER DESIGN MODEL

To achieve rapid and efficient calibration of ORS parameters, shorten the product development cycle, reduce simulation computational overhead, and thereby improve overall development efficiency, this paper constructs a concise and efficient intelligent parameter solving method. Building on the multimodal dataset constructed and preprocessed in Chapter 3, this chapter proposes the ORS-PDM model framework and elaborates on its network architecture, training scheme, and evaluation metrics one by one.

4.1 Network Architecture Design

To effectively process the three types of heterogeneous modality inputs—the crash pulse, the head acceleration-time curve, and the grayscale image of the spatial layout—ORS-PDM adopts ShuffleNet V2 as the backbone network. Through channel split and depthwise separable convolution designs, this architecture can capture nonlinear features in high-dimensional inputs even with a limited number of parameters, balancing multimodal feature extraction capability with the inference efficiency required for engineering deployment.

Channel fusion of multimodal inputs: After preprocessing in Chapter 3, the three modalities have been respectively converted into tensor representations of unified size: the crash pulse and head acceleration-time curve are retained as time-series channels, and the spatial layout information is encoded as a single-channel grayscale image. The above channels are directly concatenated in terms of dimensions to form a multi-channel joint input tensor $X_{fusion} \in R^{\{C\times H\times W\}}$, where $C = C_{time} + 1$ (C_{time} is the number of time-series channels, and 1 is the grayscale image channel). The concatenated tensor simultaneously carries temporal dynamics and spatial structure information and serves as a single input for forward propagation of the network.

Overview of the model structure: The structure of ORS-PDM is shown in the Figure 6.

Among them, the basic ShuffleNet V2 unit is divided into two modes according to stride: when stride = 1, channel split is adopted, dividing the input features into two parts c-c' and c' (in this study, $c'=c/2$ for equal split); one branch is directly passed through, while the other branch extracts features via depthwise separable convolution, and the two branches are fused through concatenation rather than element-wise addition to retain more feature information. When stride = 2, channel split is omitted, the right branch still maintains depthwise separable convolution to reduce computational cost, and the left branch performs downsampling to adjust feature size. The overall architecture of the model is shown in Figure 6.

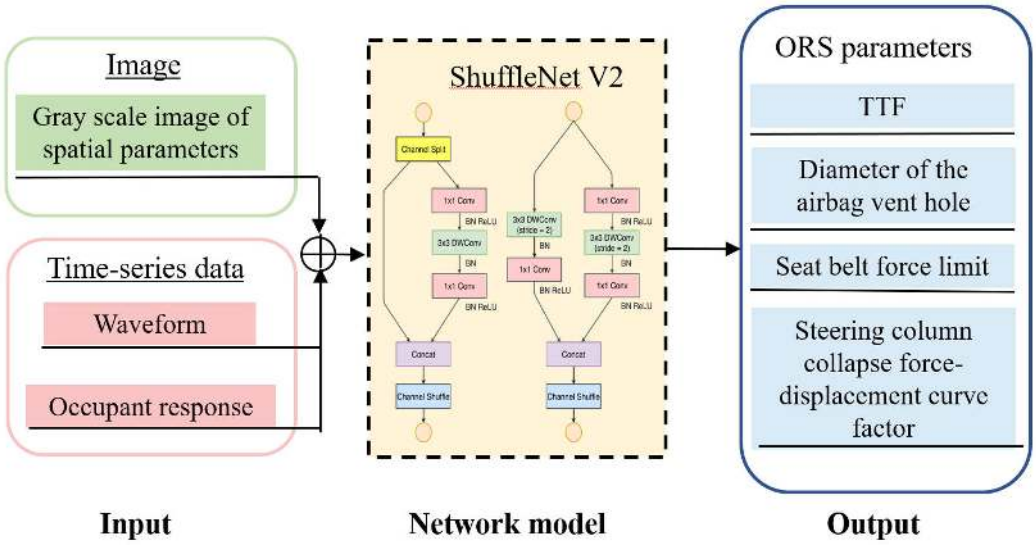


Figure 6 ORS-PDM framework.

4.2 Model Training.

4.2.1 Training Parameters

Loss function: The output of ORS-PDM consists of four continuous ORS design parameters, which is a multi-output regression task. Therefore, Mean Squared Error (MSE) is adopted as the loss function:

$$L_{MSE} = \frac{1}{n}\sum_{i=1,j=1}^{n}\left(y_{i,j} - \hat{y}_{i,j}\right)^2 \tag{3}$$

where *N* is the batch size, and $y_{i,j}$ and $\hat{y}_{i,j}$ denote the ground-truth and predicted values of the j-th parameter for the *i-th* sample, respectively. MSE imposes a squared penalty on large deviations, causing the model to prioritize correcting parameters with larger prediction deviations during training. Before training, the four output parameters are mapped to [0, 1] via min-max normalization, and the loss is computed in the normalized space; after prediction is completed, the output values are inverse-normalized back to physical dimensions.

Optimizer and hyperparameters: Model training adopts the Adaptive Moment Estimation (Adam) optimizer. Adam simultaneously utilizes the first moment estimate (momentum) and the second moment estimate (adaptive learning rate) of the gradient, and exhibits good convergence characteristics in non-stationary objective and non-stationary gradient scenarios. The initial learning rate and weight decay coefficient are set to 1×10^{-4} and 1×10^{-3} , respectively. The model is trained for 1,000 epochs with a batch size of 2.

Weight decay is applied only to the weights of convolutional layers and fully connected layers; bias terms and Batch Normalization parameters are not subject to it, to avoid undue interference with normalization statistics. All models are trained on an NVIDIA GeForce RTX 4090 GPU with 24 GB of video memory.

4.2.2 K-Fold Cross-Validation

To fully evaluate the generalization ability of the model and reduce the accidental bias caused by a single data split, this study adopts five-fold cross-validation. The complete dataset is uniformly divided into five mutually exclusive subsets. In each fold, one subset is rotated as the test set, and the remaining four subsets are merged as the training set, i.e., the training/test ratio for each fold is 80%/20%. Each fold independently completes the full training process (random weight initialization → 1000 epochs of iteration) and computes evaluation metrics on the corresponding test set. Finally, the mean of the five-fold metrics is taken as the overall estimate of the model's generalization performance, and the fluctuation amplitude among folds is used to measure the model's stability with respect to data splitting.

The choice of five-fold cross-validation is mainly based on the following two points: (1) The current dataset size is limited, and a single fixed split may make the evaluation results overly dependent on the composition of a specific subset; five-fold rotation ensures that each sample participates in both training and evaluation, maximizing data utilization. (2) The dispersion of metrics across folds directly reflects the model's performance consistency under different data distributions, providing a quantitative basis for evaluating the model's robustness.

4.3 Evaluation Metrics

During training, the goal of ORS-PDM is to accurately learn the nonlinear mapping relationship between occupant responses and the corresponding optimal restraint system parameters. To evaluate the predictive performance and practical effectiveness of the proposed model, a simulation-based validation process is adopted. After ORS-PDM predicts the ORS parameters, these parameters are input into the validated MADYMO multi-rigid body simulation environment to compute the corresponding occupant kinematic responses and injury assessment metrics. These output results are hereinafter collectively referred to as the "designed occupant response" and "designed injury metrics." The similarity between the designed output and the target output is defined as "design accuracy," which is a key metric for measuring the practical application value of the model.

Given the multimodal nature of the data, different evaluation strategies are employed for time-series and scalar outputs:

6. For time-series data (e.g., head acceleration-time curves), evaluation is performed in accordance with the ISO/TS 18571 standard. This method decomposes the total crash pulse error into four components: corridor error, phase error, magnitude error, and morphology error; a weighted composite score E is then computed to quantify the overall similarity between the predicted curve and the target curve.

7. For scalar injury metrics (e.g., HIC15, 3 ms acceleration), model performance is quantified using Root Mean Squared Error (RMSE) and prediction accuracy. These metrics are defined as follows:

$$\mathrm{RMSE} = \sqrt{\mathrm{MSE}} = \sqrt{\frac{\sum(\mathrm{y_i}-\hat{\mathrm{y}}_\mathrm{i})^2}{\mathrm{n}}} \quad (4)$$

$$\mathrm{accuracy} = 1 - \frac{100\%}{\mathrm{n}} \times \mathrm{MAE} = 1 - \frac{100\%}{\mathrm{n}} \times \frac{\sum|\mathrm{y_i}-\hat{\mathrm{y}}_\mathrm{i}|}{\mathrm{y_i}} \quad (5)$$

where, y_i denotes the real value, $\hat{y}_i$ denotes the predicted value obtained by the ORS-PDM, n denotes the number of samples in the dataset.

5. RESULTS AND DISCUSSION

5.1 Evaluation of ORS-PDM via Five-Fold Cross-Validation

To evaluate the generalization ability and robustness of the proposed ORS-PDM model, a five-fold cross-validation was conducted using the full dataset. The results are summarized in Table 4. Each fold produced slightly different design outputs, indicating that the model exhibits a modest sensitivity to the specific data partitioning. Despite these differences, the maximum variation in prediction accuracy for the HIC and the comprehensive crash pulse similarity score E across the five folds was only 3.54%. This minor fluctuation indicates that the ORS-PDM maintains high prediction accuracy and consistency across varying data splits. The consistently strong performance across folds demonstrates that the model is both stable and reliable, making it well-suited for engineering applications where robust parameter prediction is essential.

Table 2. Five-fold cross-validation result

k-fold	HIC		Cumulative 3ms resultant acceleration		E
	accuracy	RMSE	accuracy	RMSE	
K1	0.9223	362.89	0.9783	30.89	0.9421
K2	0.8650	456.23	0.9640	41.71	0.9254
K3	0.8766	714.84	0.9598	130.58	0.9255
K4	0.8777	564.85	0.9635	49.66	0.9293
K5	0.9124	285.19	0.9718	38.78	0.9426
average	0.8908	476.80	0.9675	58.32	0.9330

5.2 Comparative evaluation of CNN architectures for ORS parameter design

To verify the effectiveness and efficiency of ShuffleNet V2 in the ORS parameter design task, this section compares its performance with three commonly used convolutional neural networks (CNNs): ResNet18, ResNet50, and MobileNet V2. All models were trained under the same conditions using the dataset established in Section 3, and their performance was systematically assessed in terms of accuracy, computational efficiency, and training stability.

ResNet architectures are widely used deep learning models known for their residual learning blocks, which address the degradation problem in very deep networks. ResNet18, which adopts BasicBlocks, and ResNet50, which adopts deeper Bottleneck structures, were selected to explore the impact of model depth and residual structure on prediction performance. In contrast, MobileNet V2 is a lightweight network designed for embedded and mobile applications. It incorporates depthwise separable convolutions and inverted residual blocks with linear bottlenecks, significantly reducing computational cost while maintaining reasonable accuracy.

To ensure a fair comparison, all models were trained using the same hyperparameters and training protocol, summarized in Table 2.To ensure a fair comparison, all models were trained using the same training protocol and hyperparameter settings. Specifically, each model was trained for 1,000 epochs using the Adam optimizer, with an initial learning rate of 1×10^{-3} and a weight decay coefficient of 1×10^{-2}.

The dataset was divided into 80% training and 20% validation sets. Figure 7 illustrates the training loss curves ofthe four CNNs. All models show a rapid decline in loss followed by stabilization ResNet50 experienced a plateau between epochs 0–200 due to local minima but eventually converged. However, MobileNet V2 plateaued at a relatively high loss, indicating it may have fallen into a local optimum.

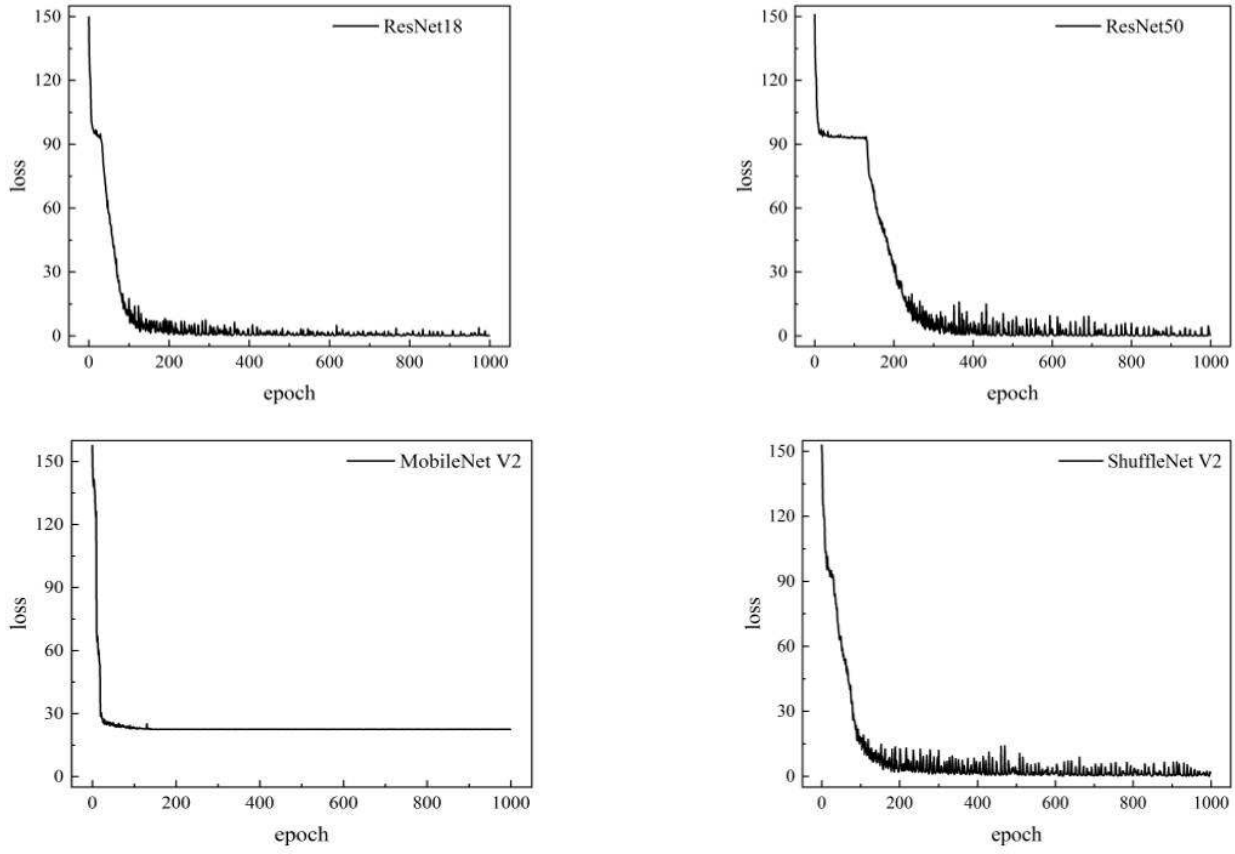


Figure 7 Training loss curves of the four models.

Table 3 shows that MobileNet V2 and ShuffleNet V2 were significantly more efficient than the deeper ResNet variants. ShuffleNet V2 achieved a strong balance, requiring only 161 minutes to complete 1000 epochs, significantly less than ResNet18 (371 minutes) and ResNet50 (493 minutes)

Table 3. The required time of different CNNs

CNN	time
ResNet18	371min
ResNet50	493min
MobileNet V2	155min
ShuffleNet V2	161min

To visualize prediction quality, selected results of the head acceleration–time response are shown in Figure 8. The black curve represents the target occupant response, while the red curve is the model-predicted response. ShuffleNet V2, ResNet18, and ResNet50 closely matched the target curves. In contrast, MobileNet V2 produced largerdeviations in both shape and magnitude.

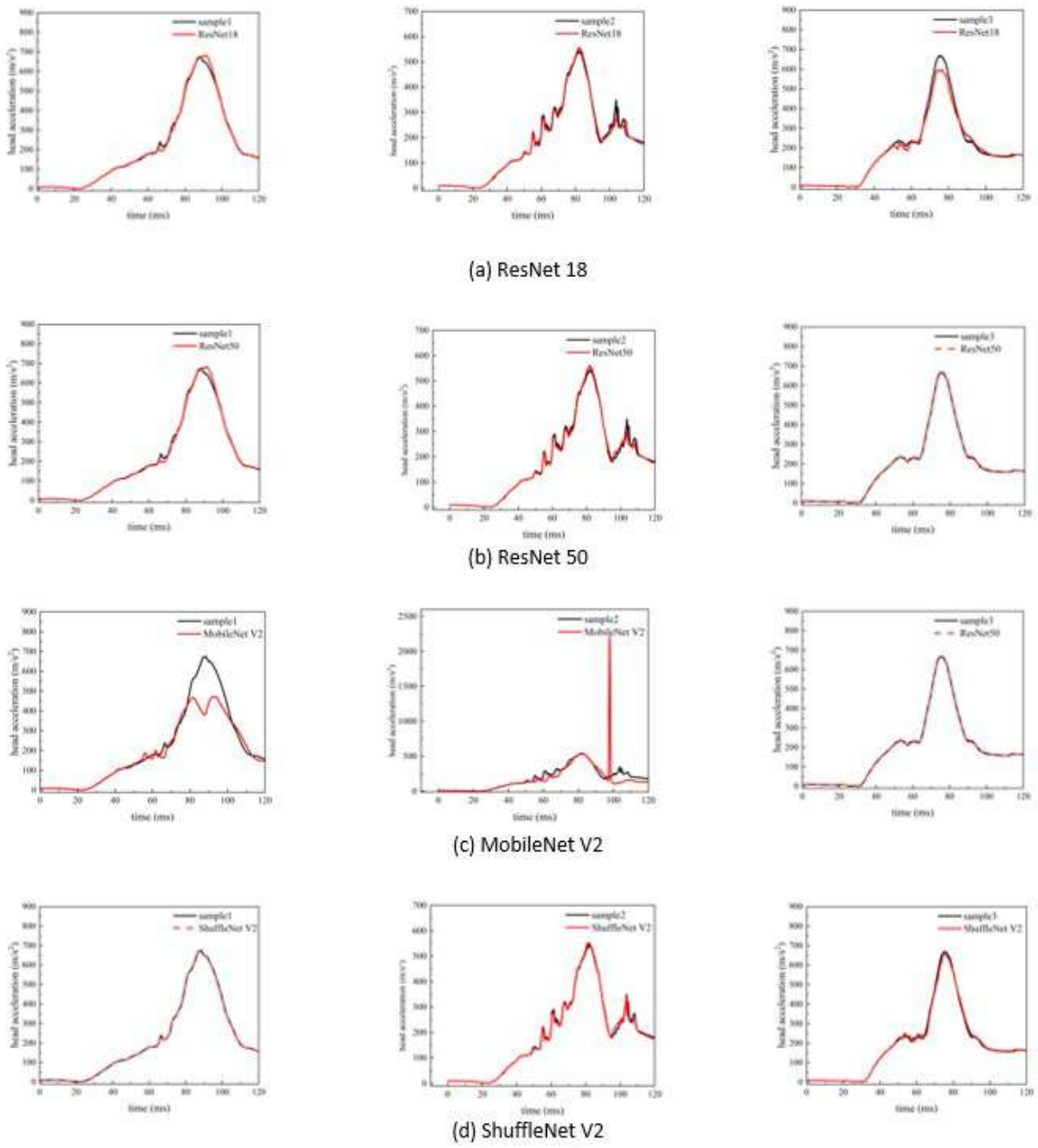


Figure 8 Some of the results on the validation dataset

The performance metrics on the validation dataset are shown in Table 4.The design accuracy of MobileNet V2 for HIC is only 0.6423, and the RMSE reaches 828.36, while the other metrics are also in the worst state of the four CNNs. Given that the stabilized loss value of MobileNet V2 is highest, we concluded MobileNet V2 falled into the local optimum and was unsuitable to be applied to the design of the ORS parameters in this study. The difference between ResNet18 and ResNet50 in the design accuracy of each assessment indicators is less than 0.015, bnd the time used to train the model under the same conditions of ResNet18 is 75% of that of ResNet50 due to the fewer number of layers in the network. ShuffleNet V2 has the highest prediction accuracy for HIC and cumulative 3ms resultant acceleration, and the RMSE value is significantly lower than the other three CNN models. In addition, the training of1000 steps for ShuffleNet V2 model only takes 161min, which is 43.4% of the time consumed by ResNet18, and 32.66% of the time consumed by ResNet50, so ShuffleNet V2 was chosen in this paper.

Quantitative performance results are summarized in Table 6. ShuffleNet V2 achieved the highest accuracy in both HIC and cumulative 3 ms resultant acceleration, with significantly lower RMSE values compared to other models. ResNet18 and ResNet50 performed comparably, with only slight differences in accuracy. However, MobileNet V2 underperformed across all metrics, supporting the hypothesis that it was trapped in a suboptimal solution space during training.

Table 4. The performance metrics on the validation dataset

ORS-PDM	HIC		Cumulative 3ms resultant acceleration		E
	accuracy	RMSE	accuracy	RMSE	
ResNet18	0.9094	506.16	0.9729	44.51	0.9475
ResNet50	0.8962	545.69	0.9715	35.87	0.9394
MobileNet V2	0.6423	828.36	0.8953	88.19	0.8486
ShuffleNet V2	0.9223	362.89	0.9783	30.89	0.9421

Based on these results, ShuffleNet V2 emerged as the most effective model, offering superior prediction accuracy, minimal computational cost, and robustness during training. Its ability to generalize well with minimal time and resource consumption makes it particularly suitable for rapid, real-time applications in occupant restraint system design.

5.3 Application example

To further validate the practical applicability of the proposed ORS-PDM model, an application example was conducted using a vehicle scenario (referred to as Vehicle A) that was not included in the model's training dataset. Based on prior engineering investigations, a desirable head acceleration–time response had previously been achieved through iterative simulations and tuning. This response, shown as the target curve in Figure 9 , demonstrated excellent protection performance and was therefore selected as the design target in this study. The objective was to test whether the ORS-PDM could efficiently reproduce this target occupant response through a direct, data-driven prediction of ORS parameters.

Table 5. Parameters designed by ORS-PDM

parameters	the value designed by ORS-PDM
TTF	16ms
diameter of the airbag vent hole	36mm
seat belt force limit	4500N
steering column collapse force-displacement curve factor	0.3

During the development of Vehicle A, the frontal crash pulse was obtained through full-scale crash testing The initial configuration of the occupant restraint system and the seating posture of the dummy were documented and represented as a grayscale spatial parameter image. These two inputs were then fed into the trained ORS-PDM model, with the head acceleration–time curve from a prior physical test set as the design target. Within only 75.326 ms, the model generated a set of optimized ORS parameters capable of reproducing the desired occupant response. The predicted parameter values are summarized in Table 5.

To evaluate the quality of the predicted parameters, a full vehicle simulation was carried out using the MADYMO multibody dynamics platform. The head acceleration–time curve resulting from the ORS-PDM design is plotted against the original design target in Figure 9. The two curves exhibit excellent agreement in both amplitude and shape, and the overall crash pulse similarity score E reached 0.9508, indicating a high-quality match. In terms of quantitative injury assessment, Table 6 summarizes the comparison between the target and predicted head injury metrics. The predicted values of HIC and cumulative 3 ms resultant acceleration were very close to the target, with respective accuracies of 0.9610 and 0.9776.

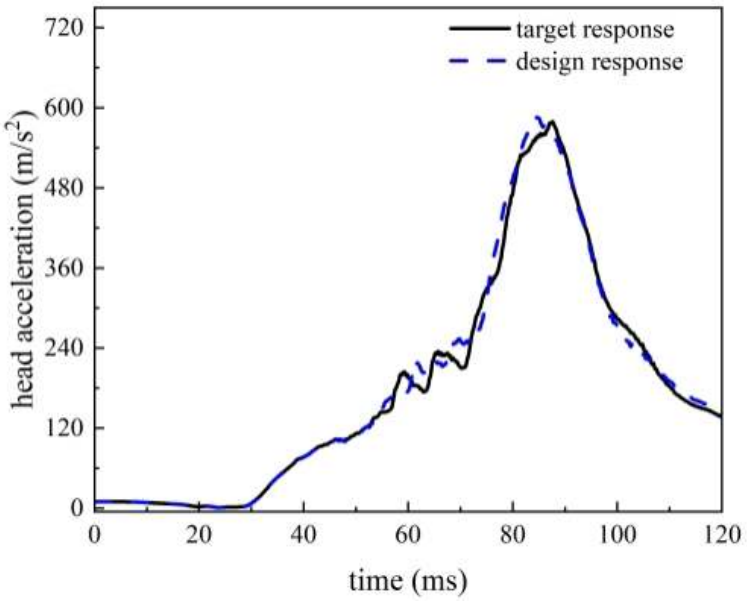


Figure 9 The target and design head acceleration.

Table 6. The target and design head assessment indicators

head assessment indicators	target value	design value	accuracy
HIC	307.41	319.38	0.9610
Cumulative 3ms resultant acceleration	559.91	572.46	0.9776

6. CONCLUSION

This paper proposes an inverse design method for ORS parameters oriented to frontal crash conditions. The model builds the ORS-PDM based on ShuffleNet V2, achieving unified input and joint representation of multimodal parameters including time-series, image, and numerical data: three types of heterogeneous modality data—the crash pulse (time-series modality), the grayscale image of the human-machine layout (image modality), and the HIC metric (numerical modality)—are taken as inputs; after unified preprocessing, the three modalities are encoded into tensor channels, concatenated at the channel level, and fed into the model, thereby realizing the inverse design of ORS parameters.

In terms of prediction accuracy, under five-fold cross-validation, the restraint parameters designed by ORS-PDM achieve average prediction accuracies of 0.8908, 0.9675, and 0.9330 for HIC, cumulative 3 ms resultant acceleration, and the composite curve similarity score E, respectively, with small fluctuations among folds, indicating that the model has good prediction accuracy and generalization stability. In terms of computational efficiency, the model generates a set of optimized ORS parameters in only 75.326 ms, compared with traditional methods that rely on iterative simulation and manual parameter tuning, which can take hours. Meanwhile, in the unseen application case of Vehicle A, verified by MADYMO multi-rigid body simulation, the head response reproduced by the model-designed parameters is highly consistent with the design target (the accuracies of HIC and cumulative 3 ms resultant acceleration are 0.9610 and 0.9776, respectively, and the composite similarity score E is 0.9508). Taken together, the proposed method compresses the parameter design cycle from hours of traditional iterative simulation to the millisecond level while ensuring prediction accuracy, balancing both accuracy and efficiency, and has significant engineering application value in the early development and virtual validation of real-vehicle restraint systems. The current dataset still covers only a limited number of design parameters, vehicle models, crash modes, and dummy types, and takes the head response as the sole design target.

Future work will expand the data coverage and extend the design target to multi-objective injury criteria for multiple body regions, to more comprehensively support the development and validation of real-vehicle restraint systems.

Author's Contributions: Investigation, Hongbin Tang, Ledan Liu; Methodology, Hongbin Tang, Ledan Liu; Conceptualization, Hongbin Tang, Jian Xie; Writing - Reviewing & Editing, Ledan Liu,; Writing Original draft, Hongbin Tang, Jian Xie.

Data availability statement: Research data is not available

Editor: Marcilio Alves.

References

Chen, G., Link, T. M., Shi, M. F., & Tyan, T. (2013). Modeling of material orientation effects on AHSS crush and fracture behavior in axial crush tests. Traffic Injury Prevention, 14(Suppl. 1), S23–S29. https://doi.org/10.1080/15389588.2013.790537

China Automotive Technology and Research Center (CATARC). (2024). C-NCAP management regulation (2024 Edition). Retrieved from http://www.c-ncap.org/

Deguchi, T., Tatsu, K., Saeki, H., & Okabe, T. (2013). Design sensitivity study of passenger airbag shape to meet head restraint performance for different occupant size in frontal impact. In Proceedings of the 23rd International Technical Conference on the Enhanced Safety of Vehicles (ESV), Seoul, Korea.

Dubois, D., Zellmer, H., & Markiewicz, E. (2009). Experimental and numerical analysis of seat belt bunching phenomenon. International Journal of Impact Engineering, 36(6), 763–774. https://doi.org/10.1016/j.ijimpeng.2008.11.006

Esat, V. (2014). Injury criteria based optimisation of automobile passive safety systems to mitigate the effects of full-frontal automobile collisions. In Proceedings of the ASME 2014 12th Biennial Conference on Engineering Systems Design and Analysis (ESDA2014), Copenhagen, Denmark. https://doi.org/10.1115/ESDA2014-20159

Gu, X., Sun, G., Li, G., Huang, X., Li, Y., & Li, Q. (2013). Multiobjective optimization design for vehicle occupant restraint system under frontal impact. Structural and Multidisciplinary Optimization, 47(3), 465–477. https://doi.org/10.1007/s00158-012-0811-7

He, K., Zhang, X., Ren, S., & Sun, J. (2016). Deep residual learning for image recognition. In Proceedings of the IEEE Conference on Computer Vision and Pattern Recognition (CVPR), pp. 770–778. https://doi.org/10.1109/CVPR.2016.90

Heo, J., Cho, M. G., & Kim, T. (2024). Optimization of occupant restraint system using machine learning for THOR-M50 and Euro NCAP. Machines, 12(1), 74. https://doi.org/10.3390/machines12010074

Horii, H. (2017). Multi-objective optimization of vehicle occupant restraint system by using evolutionary algorithm with response surface model. International Journal of Computational Methods and Experimental Measurements, 5(2), 163–170. https://doi.org/10.2495/CMEM-V5-N2-163-170

International Organization for Standardization. (2014). Road vehicles — Objective rating metric for non-ambiguous signals. ISO/TS 18571.

Ito, O., et al. (2019). Prediction of pedestrian protection performance using machine learning. In Proceedings of the 26th International Technical Conference on the Enhanced Safety of Vehicles (ESV), Eindhoven, the Netherlands.

Keleko, A. T., Kamsu-Foguem, B., Ngouna, R. H., & Tongne, A. (2023). Health condition monitoring of a complex hydraulic system using deep neural network and DeepSHAP explainable XAI. Advances in Engineering Software, 175, Article 103339. https://doi.org/10.1016/j.advengsoft.2022.103339

Lee, S., Lee, T., et al. (2021). Pedestrian head injury prediction based on vehicle section image using machine learning. In Proceedings of the FISITA World Congress 2021 (virtual), Paper No. F2021-PIF-066.

Li, Z., Zhang, J., Lai, Q., & Ma, C. (2012). Development and optimization of a new occupant restraint system for improving mini vehicle safety. In Proceedings of ICTIS 2011, pp. 1985–1992. https://doi.org/10.1061/41177(415)250

Li, Z., Ma, W., Yao, S., Xu, P., Hou, L., & Deng, G. (2021). A machine learning based optimization method towards removing undesired deformation of energy-absorbing structures. Structural and Multidisciplinary Optimization, 64(2), 919–934. https://doi.org/10.1007/s00158-021-02896-1

Liu, C. H., Lai, Y. C., Chiu, C. H., & Lin, M. H. (2016). Interior head impact analysis of automotive instrument panel for unrestrained front seat passengers. Key Engineering Materials, 715, 186–191. https://doi.org/10.4028/www.scientific.net/KEM.715.186

Liu, Q., Wu, X., Han, X., Liu, J., Zhang, Z., & Guo, S. (2019). Sensitivity analysis and interval multi-objective optimization for an occupant restraint system considering craniocerebral injury. Journal of Mechanical Design, 142(2), Article 024502. https://doi.org/10.1115/1.4044328

Ma, N., Zhang, X., Zheng, H.-T., & Sun, J. (2018). ShuffleNet V2: Practical guidelines for efficient CNN architecture design. In Computer Vision — ECCV 2018, Part XIV, pp. 122–138. Springer. https://doi.org/10.1007/978-3-030-01264-9_8

Mathieu, J., Gupta, P., Di Roberto, M., & Vielhaber, M. (2024). Minimizing occupant loads in vehicle crashes through reinforcement learning-based restraint system design: assessing performance and transferability. Proceedings of the Design Society, 4, 2139–2148. https://doi.org/10.1017/pds.2024.216

Pachocki, L., & Fang, H. (2024). Numerical modelling of different airbag folding patterns and their influence on occupant responses in frontal vehicle impact. International Journal of Crashworthiness, 29(6), 1035–1050. https://doi.org/10.1080/13588265.2024.2348381

Parenteau, C. (2006). A comparison of volunteers and dummy upper torso kinematics with and without shoulder belt slack in a low speed side/pre-roll environment. Traffic Injury Prevention, 7(2), 155–163. https://doi.org/10.1080/15389580500481973

Radu, A. I., Cofaru, C., Tolea, B., & Dima, D. (2018). Study regarding the influence of airbag deployment time on the occupant injury level during a frontal vehicle collision. MATEC Web of Conferences, 184, Article 01007. https://doi.org/10.1051/matecconf/201818401007

Rezapour, M., Nazneen, S., & Ksaibati, K. (2020). Application of deep learning techniques in predicting motorcycle crash severity. Engineering Reports, 2(7), e12175. https://doi.org/10.1002/eng2.12175

Sameen, M. I., & Pradhan, B. (2017). Severity prediction of traffic accidents with recurrent neural networks. Applied Sciences, 7(6), 476. https://doi.org/10.3390/app7060476

Siegmund, G. P., Chimich, D. D., Heinrichs, B. E., DeMarco, A. L., & Brault, J. R. (2005). Variations in occupant response with seat belt slack and anchor location during moderate frontal impacts. Traffic Injury Prevention, 6(1), 38–43. https://doi.org/10.1080/15389580590903159

Wang, Q., Gan, S., Chen, W., Li, Q., & Nie, B. (2021). A data-driven, kinematic feature-based, near real-time algorithm for injury severity prediction of vehicle occupants. Accident Analysis & Prevention, 156, Article 106149. https://doi.org/10.1016/j.aap.2021.106149

Wang, Q., Li, R., Shang, S., Zhou, Q., & Nie, B. (2024). A lightweight pre-crash occupant injury prediction model distills knowledge from its post-crash counterpart. Journal of Biomechanical Engineering, 146(3), Article 031004. https://doi.org/10.1115/1.4063033

Xiang, Z., & Xiang, F. (2023). Multi-parameter and multi-objective optimization of occupant restraint system in frontal collision. Wuhan University Journal of Natural Sciences, 28(4), 324–332. https://doi.org/10.1051/wujns/2023284324

Xie, J., Zhang, J., Dou, Z., Chang, M., & Su, C. (2025). An explainable machine learning method for predicting and designing crashworthiness of multi-cell tubes under oblique load. Engineering Applications of Artificial Intelligence, 147, Article 110396. https://doi.org/10.1016/j.engappai.2025.110396

Yang, X., Shi, J., Fu, Q., Pu, S., Pan, Z., Lian, C., Yin, Z., Liu, S., & Wang, G. (2022). Optimization design and injury analysis of driver's restraint system in sedan small offset collision. Processes, 10(5), Article 940. https://doi.org/10.3390/pr10050940

Yang, Z., Desai, A., Boyle, K., Rupp, J., Reed, M., & Hu, J. (2023). Restraint system optimizations using diverse human body models in frontal crashes. SAE International Journal of Transportation Safety, 11(2), 187–195. https://doi.org/10.4271/09-11-02-0018

Zhang, J. (2003). Research on optimization of parameters and system performance stability of microbus occupant restraint system (Ph.D. thesis). Changchun, China: Jilin University.

Zhang, J., Jin, Y., Xie, L., & Chen, C. (2015). Establishment and validation for the theoretical model of the vehicle airbag. Chinese Journal of Mechanical Engineering, 28(3), 487–495. https://doi.org/10.3901/CJME.2015.0312.029

Zhang, J. (2018). Parameter design method for structure and occupant restraint system in vehicle crash. Beijing, China: Science Press.

Zhang, J., Wang, D., Ni, Y., & Chen, C. (2019). A two degrees of freedom model-based optimization method for occupant restraint systems in vehicle crash. Structural and Multidisciplinary Optimization, 60(6), 2597–2614. https://doi.org/10.1007/s00158-019-02340-5

Zhang, S., Zhu, D., & Zhai, G. (2022). Prediction on seat's anti-whiplash-injury performance based on deep learning. Automotive Engineering, 44(10), 1600–1608. https://doi.org/10.19562/j.chinasae.qcgc.2022.10.015

Zhang, X., Zhou, X., Lin, M., & Sun, R. (2018). ShuffleNet: An extremely efficient convolutional neural network for mobile devices. In Proceedings of the IEEE/CVF Conference on Computer Vision and Pattern Recognition (CVPR), pp. 6848–6856. https://doi.org/10.1109/CVPR.2018.00716

Zhou, H., Zhong, Z., & Hu, M. (2018). Design and occupant-protection performance analysis of a new tubular driver airbag. Engineering, 4(2), 291–297. https://doi.org/10.1016/j.eng.2018.03.015